

# Outage Analysis of Cooperative NOMA in Millimeter Wave Vehicular Network at Intersections

Baha Eddine Youcef Belmekki<sup>1,2</sup>, Abdelkrim Hamza<sup>1</sup>, and Benoît Escrig<sup>2</sup>

<sup>1</sup>LISIC Laboratory, Electronic and Computer Faculty, USTHB, Algiers, Algeria,  
email: {bbelmekki, ahamza}@usthb.dz

<sup>2</sup>University of Toulouse, IRIT Laboratory, School of ENSEEIHT, Institut National Polytechnique de Toulouse, France, e-mail: {bahaeddine.belmekki, benoit.escrig}@enseeiht.fr

## Abstract

In this paper, we study the impact and the improvement of using cooperative non-orthogonal multiple access scheme (NOMA) on a millimeter wave (mmWave) vehicular network at intersection roads. The intersections consists of two perpendicular roads. The transmission occurs between a source, and two destinations nodes with a help of a relay. We assume that the interference comes from as set of vehicles that are distributed as a one dimensional homogeneous Poisson point process (PPP). We derive closed form outage probability expressions for cooperative NOMA, and compare them with cooperative orthogonal multiple access (OMA). We show that, NOMA offers a significant improvement, especially for high data rates. However, there a condition imposed to the data rate, otherwise, the performance of NOMA will decreases dramatically. We show that as the nodes approach the intersection, the outage probability increases. Counter-intuitively, We show that, the non line of sigh (NLOS) scenario has a better performance than the line of sigh (LOS) scenario. The analysis is conducted using tools from stochastic geometry and is verified with Monte Carlo simulations.

## Index Terms

5G, NOMA, mmWave, interference, outage probability, cooperative, vehicular communications.

### A. Motivation

Road traffic safety is a major issue, and more particularly at intersections [1]. Vehicular communications offer several applications for accident prevention, or alerting vehicles when accidents happen in their vicinity. High reliability and low latency communications are required in safety-based vehicular communications. To increase the data rate and spectral efficiency [2] in the fifth generation (5G) of communication systems, non-orthogonal multiple access (NOMA) is an appropriate candidate as a multiple access scheme. Unlike orthogonal multiple access (OMA), NOMA allows multiple users to share the same resource with different power allocation levels. In the other hand, the needs of the 5G in terms of resources require a large bandwidth, since the spectral efficiency of sub-6 GHz bands has already reached the theoretical limits. To cope with this limitation, millimeter wave (mmWave) frequency bands (20-100 GHz and beyond) offer a very large bandwidth [3].

### B. Related works

1) *Cooperative NOMA*: NOMA is an efficient multiple access technique for spectrum use. It has been shown that NOMA outperforms OMA [4]–[8]. However, few research investigates the effect of co-channel interference and their impact on the performance considering direct transmission [9]–[11], and cooperative transmission [12].

2) *Cooperative mmWave*: In mmWave bands, few works studied cooperative communications using tools from stochastic geometry [13]–[16].

In [13] and [14], the authors used one way cooperative transmission using amplify and forward protocol. In [15], the authors show improvement of two-way cooperative transmission. However, in [13]–[15], the effect of small-scale fading is not taken into consideration. In [16], the authors investigate the performance of mmWave relaying network in terms of coverage probability with best relay selection.

3) *Vehicular communications*: Regarding vehicular communications, several works took into account the effect of interference considering OMA in highway scenarios [17]. As for intersection scenarios, the performance in terms of success probability are derived [18], [19]. The performance of vehicle to vehicle (V2V) communications are evaluated for multiple intersections scheme in [20]. In [21], the authors derive the outage probability of a V2V communications with power control strategy.

Following this line of research, we study the performance of vehicular communications at intersections in the presence of interference. However, all the works that study intersections neither consider NOMA nor cooperative transmissions. Plus, no previous works have investigated the performance of cooperative NOMA in a mmWave vehicular network.

At the best of the author's knowledge, there are no prior works that consider an intersection scenario with cooperative transmissions using NOMA and considering mmWave network. Our analysis includes the effects of blockage from the building in intersections, and Nakagami- $m$  fading channels between the transmitting nodes with difference values of  $m$  for LOS and NLOS are considered.

### C. Contributions

The contributions of this paper are as follows:

- We study the impact and the improvement of using cooperative NOMA on a mmWave vehicular network at intersection roads. Closed form expressions of the outage probability are obtained.
- Our analysis includes the effects of blockage from the building in intersections, and Nakagami- $m$  fading channels with difference values of  $m$  for LOS and NLOS are considered.
- We evaluate the performance of NOMA for both intersection, and show that the outage probability increases when the vehicles move toward the intersections. We also show the effect of LOS and NLOS on the performance at the intersection.
- We compare all the results obtained with cooperative OMA, and show that cooperative NOMA is superior in terms of outage probability than OMA.

## I. SYSTEM MODEL

### A. Scenario model

In this paper, we consider a mm-Wave vehicular network using a cooperative NOMA transmission between a source, denoted  $S$ , and two destinations denoted  $D_1$  and  $D_2$  with the help of a relay denoted  $R$ . The set  $\{S, R, D_1, D_2\}$  denotes the nodes and their locations as depicted in Fig.1.

We consider an intersection scenario involving two perpendicular roads, an horizontal road denoted by  $X$ , and a vertical road denoted by  $Y$ . In this paper, we consider both V2V and V2I

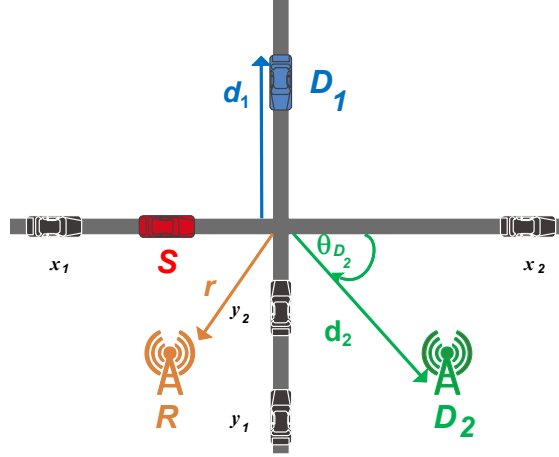


Fig. 1: Cooperative NOMA system model for vehicular communications involving one relay two receiving node. The receiving nodes can be vehicles or as part of the communication infrastructure. For instance,  $S$  and  $D_1$  are vehicles, and  $R$  and  $D_2$  are infrastructures.

communications<sup>1</sup>, hence, any node of the set  $\{S, R, D_1, D_2\}$  can be on the road or outside the roads. We denote by  $M$  the receiving node, and by  $m$  the distance between the node  $M$  and the intersection, where  $M \in \{R, D_1, D_2\}$  and  $m \in \{r, d_1, d_2\}$ , as shown in Fig.1. The angle  $\theta_M$  is the angle between the node  $M$  and the  $X$  road (see Fig.1). Note that the intersection is the point where the  $X$  road and the  $Y$  road intersect. The set  $\{S, R, D_1, D_2\}$  is subject to interference that are originated from vehicles located on the roads.

The set of interfering vehicles located on the  $X$  road that are in a LOS with  $\{S, R, D_1, D_2\}$ , denoted by  $\Phi_X^{\text{LOS}}$  (resp. on axis  $Y$ , denoted by  $\Phi_Y^{\text{LOS}}$ ) are modeled as a One-Dimensional Homogeneous Poisson Point Process (1D-HPPP), that is,  $\Phi_X^{\text{LOS}} \sim \text{1D-HPPP}(\lambda_X^{\text{LOS}}, x)$  (resp.  $\Phi_Y^{\text{LOS}} \sim \text{1D-HPPP}(\lambda_Y^{\text{LOS}}, y)$ ), where  $x$  and  $\lambda_X^{\text{LOS}}$  (resp.  $y$  and  $\lambda_Y^{\text{LOS}}$ ) are the position of the LOS interferer vehicles and their intensity on the  $X$  road (resp.  $Y$  road).

Similarly, the set of interfering vehicles located on the  $X$  road that are in a NLOS with  $\{S, R, D_1, D_2\}$ , denoted by  $\Phi_X^{\text{NLOS}}$  (resp. on axis  $Y$ , denoted by  $\Phi_Y^{\text{NLOS}}$ ) are modeled as a One-Dimensional Homogeneous Poisson Point Process (1D-HPPP), that is,  $\Phi_X^{\text{NLOS}} \sim \text{1D-HPPP}(\lambda_X^{\text{NLOS}}, x)$  (resp.  $\Phi_Y^{\text{NLOS}} \sim \text{1D-HPPP}(\lambda_Y^{\text{NLOS}}, y)$ ), where  $x$  and  $\lambda_X^{\text{NLOS}}$  (resp.  $y$  and  $\lambda_Y^{\text{NLOS}}$ ) are the position of the NLOS interferer vehicles and their intensity on the  $X$  road (resp.  $Y$  road). The notation  $x$  and  $y$  denotes both the interferer vehicles and their locations.

<sup>1</sup>The Doppler shift and time-varying effect of V2V and V2I channel is beyond the scope of this paper

### B. Blockage model

At the intersection, the mmWave signals cannot penetrate the buildings and other obstacles, which causes the link to be in LOS, or in NLOS. The event of a link between a node  $a$  and  $b$  is in a LOS and NLOS, are respectively defined as  $\text{LOS}_{ab}$ , and  $\text{NLOS}_{ab}$ . The LOS probability function  $\mathbb{P}(\text{LOS}_{ab})$  is used, where the link between  $a$  and  $b$  has a LOS probability  $\mathbb{P}(\text{LOS}_{ab}) = \exp(-\beta r_{ab})$  and NLOS probability  $\mathbb{P}(\text{NLOS}_{ab}) = 1 - \mathbb{P}(\text{LOS}_{ab})$ , where the constant rate  $\beta$  depends on the building size, shape and density [22].

### C. Transmission and decoding model

The transmission is subject to a path loss, denoted by  $r_{ab}^{-\alpha}$  between the nodes  $a$  and  $b$ , where  $r_{ab} = \|a - b\|$ , and  $\alpha$  is the path loss exponent. The path exponent  $\alpha \in \{\alpha_{\text{LOS}}, \alpha_{\text{NLOS}}\}$ , where  $\alpha = \alpha_{\text{LOS}}$ , when the transmission is in LOS, whereas  $\alpha = \alpha_{\text{NLOS}}$ , when transmission is in NLOS.

We consider slotted ALOHA protocol with parameter  $p$ , i.e., every node accesses the medium with a probability  $p$ .

We use a Decode and Forward (DF) decoding strategy, i.e.,  $R$  decodes the message, re-encodes it, then forwards it to  $D_1$  and  $D_2$ . We also use a half-duplex transmission in which a transmission occurs during two phases. Each phase lasts one time slot. During the first phase,  $S$  broadcasts the message to  $R$  ( $S \rightarrow R$ ). During the second phase,  $R$  broadcasts the message to  $D_1$  and  $D_2$  ( $R \rightarrow D_1$  and  $R \rightarrow D_2$ ).

### D. NOMA model

We consider in this paper, that the receiving nodes,  $D_1$  and  $D_2$ , are ordered according to their quality of service (QoS) priorities [23], [24]. We consider the case when, node  $D_1$  needs a low data rate but has to be served immediately, whereas node  $D_2$  require a higher data rate but can be served later. For instance  $D_1$  can be a vehicle that needs to receive safety data information about an accident in its surrounding, whereas  $D_2$  can be a user that accesses the internet connection.

### E. Directional beamforming model

We model the directivity similar to in [25], where the directional gain, denoted  $G(\omega)$ , within the half power beamwidth ( $\phi/2$ ) is  $G_{max}$  and is  $G_{min}$  in all other directions. The gain is then

expressed as

$$G(\omega) = \begin{cases} G_{max}, & \text{if } |\omega| \leq \frac{\phi}{2}; \\ G_{min}, & \text{otherwise.} \end{cases} \quad (1)$$

In this paper, we consider a perfect beam alignment between the nodes, hence  $G_{eq} = G_{max}^2$ . The impact of beam misalignment is beyond the scope of this paper.

#### F. Channel and interference model

We consider an interference limited scenario, that is, the power of noise is set to zero ( $\sigma^2 = 0$ ). Without loss of generality, we assume that all nodes transmit with a unit power. The signal transmitted by  $S$ , denoted  $\chi_S$  is a mixture of the message intended to  $D_1$  and  $D_2$ . This can be expressed as

$$\chi_S = \sqrt{a_1}\chi_{D1} + \sqrt{a_2}\chi_{D2},$$

where  $a_i$  is the power coefficients allocated to  $D_i$ , and  $\chi_{D_i}$  is the message intended to  $D_i$ , where  $i \in \{1, 2\}$ . Since  $D_1$  has higher power than  $D_2$ , that is  $a_1 \geq a_2$ , then  $D_1$  comes first in the decoding order. Note that,  $a_1 + a_2 = 1$ .

The signal received at  $R$  during the first time slot is expressed as

$$\begin{aligned} \mathcal{Y}_R = & h_{SR}\sqrt{r_{SR}^{-\alpha_{LOS}}}\Upsilon \chi_S \mathbb{1}(\text{LOS}_{SR}) + h_{SR}\sqrt{r_{SR}^{-\alpha_{NLOS}}}\Upsilon \chi_S \mathbb{1}(\text{NLOS}_{SR}) \\ & + \sum_{x \in \Phi_{X_R}^{\text{LOS}}} h_{Rx}\sqrt{r_{Rx}^{-\alpha_{LOS}}}\Upsilon \chi_x + \sum_{y \in \Phi_{Y_R}^{\text{LOS}}} h_{Ry}\sqrt{r_{Ry}^{-\alpha_{LOS}}}\Upsilon \chi_y \\ & + \sum_{x \in \Phi_{X_R}^{\text{NLOS}}} h_{Rx}\sqrt{r_{Rx}^{-\alpha_{NLOS}}}\Upsilon \chi_x + \sum_{y \in \Phi_{Y_R}^{\text{NLOS}}} h_{Ry}\sqrt{r_{Ry}^{-\alpha_{NLOS}}}\Upsilon \chi_y. \end{aligned}$$

The signal received at  $D_i$  during the second time slot is expressed as

$$\begin{aligned} \mathcal{Y}_{D_i} = & h_{RD_i}\sqrt{r_{RD_i}^{-\alpha}}\Upsilon \chi_S \mathbb{1}(\text{LOS}_{RD_i}) + h_{RD_i}\sqrt{r_{RD_i}^{-\alpha}}\Upsilon \chi_S \mathbb{1}(\text{NLOS}_{RD_i}) \\ & + \sum_{x \in \Phi_{X_{D_i}}^{\text{LOS}}} h_{Dix}\sqrt{r_{Dix}^{-\alpha_{LOS}}}\Upsilon \chi_x + \sum_{y \in \Phi_{Y_{D_i}}^{\text{LOS}}} h_{Diy}\sqrt{r_{Diy}^{-\alpha_{LOS}}}\Upsilon \chi_y \\ & + \sum_{x \in \Phi_{X_{D_i}}^{\text{NLOS}}} h_{Dix}\sqrt{r_{Dix}^{-\alpha_{NLOS}}}\Upsilon \chi_x + \sum_{y \in \Phi_{Y_{D_i}}^{\text{NLOS}}} h_{Diy}\sqrt{r_{Diy}^{-\alpha_{NLOS}}}\Upsilon \chi_y, \end{aligned}$$

where  $\mathcal{Y}_M$  is the signal received by  $M$ . The messages transmitted by the interfere node  $x$  and  $y$ , are denoted respectively by  $\chi_x$  and  $\chi_y$ . The term  $\Upsilon = G_{eq}\eta^2/(4\pi)^2$  models the directional gain, the reference path loss at one meter, and  $\eta$  is the wavelength of the operating frequency.

The coefficients  $h_{SR}$ , and  $h_{RD_i}$  denote the fading of the link  $S - R$ , and  $R - D_i$ . The fading coefficients are modeled as Nakagami- $m$  fading with parameter  $m$ , that is

$$f_{h_u}(x) = 2\left(\frac{m}{\mu}\right)^m \frac{x^{2m-1}}{\Gamma(m)} e^{-\frac{m}{\mu}x^2}, \quad (2)$$

where  $u \in \{SR, RD_i\}$ . The parameter  $m \in \{m_{\text{LOS}}, m_{\text{NLOS}}\}$ , where  $m = m_{\text{LOS}}$  when  $u$  is in a LOS, whereas  $m = m_{\text{NLOS}}$ , when  $u$  is in a NLOS. The parameter  $\mu$  is the average received power.

Hence, the power fading coefficients  $|h_{SR}|^2$ , and  $|h_{RD_i}|^2$  follow a gamma distribution distribution, that is,

$$f_{|h_u|^2}(x) = \left(\frac{m}{\mu}\right)^m \frac{x^{m-1}}{\Gamma(m)} e^{-\frac{m}{\mu}x}. \quad (3)$$

The fading coefficients  $h_{Rx}, h_{Ry}, h_{D_i x}$  and  $h_{D_i y}$  denote the fading of the link  $R - x$ ,  $R - y$ ,  $D_i - x$ , and  $D_i - y$ . The fading coefficients are modeled as Rayleigh fading. Thus, the power fading coefficients  $|h_{Rx}|^2$ ,  $|h_{Ry}|^2$ ,  $|h_{D_i x}|^2$  and  $|h_{D_i y}|^2$ , follow an exponential distribution with unit mean.

The aggregate interference is defined as from the  $X$  road at  $M$ , denoted  $I_{X_M}$ , is expressed as

$$I_{X_M} = I_{X_M}^{\text{LOS}} + I_{X_M}^{\text{NLOS}} = \sum_{x \in \Phi_{X_M}^{\text{LOS}}} |h_{Mx}|^2 r_{Mx}^{-\alpha_{\text{LOS}}} \Upsilon + \sum_{y \in \Phi_{X_M}^{\text{NLOS}}} |h_{My}|^2 r_{My}^{-\alpha_{\text{NLOS}}} \Upsilon, \quad (4)$$

where  $I_{X_M}^{\text{LOS}}$  denotes the aggregate interference from the  $X$  road that are in a LOS with  $M$ , and  $I_{X_M}^{\text{NLOS}}$  denotes the aggregate interference from the  $X$  road that are in a NLOS with  $M$ . Similarly,  $\Phi_{X_M}^{\text{LOS}}$  and  $\Phi_{X_M}^{\text{NLOS}}$ , denote respectively, the set of the interferers from the  $X$  road at  $M$  in a LOS, and in NLOS.

In the same way, the aggregate interference is defined as from the  $Y$  road at  $M$ , denoted  $I_{Y_M}$ , is expressed as

$$I_{Y_M} = I_{Y_M}^{\text{LOS}} + I_{Y_M}^{\text{NLOS}} = \sum_{y \in \Phi_{Y_M}^{\text{LOS}}} |h_{My}|^2 r_{My}^{-\alpha_{\text{LOS}}} \Upsilon + \sum_{y \in \Phi_{Y_M}^{\text{NLOS}}} |h_{My}|^2 r_{My}^{-\alpha_{\text{NLOS}}} \Upsilon, \quad (5)$$

where  $I_{Y_M}^{\text{LOS}}$  denotes the aggregate interference from the  $Y$  road that are in a LOS with  $M$ , and  $I_{Y_M}^{\text{NLOS}}$  denotes the aggregate interference from the  $Y$  road that are in a NLOS with  $M$ . Similarly,  $\Phi_{Y_M}^{\text{LOS}}$  and  $\Phi_{Y_M}^{\text{NLOS}}$ , denote respectively, the set of the interferers from the  $Y$  road at  $M$  in a LOS, and in NLOS.

## II. COOPERATIVE NOMA OUTAGE EXPRESSIONS

### A. Signal-to-interference (SIR) expressions

We define the outage probability as the probability that the signal-to-interference ratio (SIR) at the receiver is below a given threshold. According to successive interference cancellation (SIC) [26],  $D_1$  will be decoded first at the receiver since it has the higher power allocation, and  $D_2$  message will be considered as interference. The SIR at  $R$  to decode  $D_1$ , denoted  $\text{SIR}_{R_1}^{(\alpha)}$ , is expressed as

$$\text{SIR}_{R_1}^{(\alpha)} = \frac{|h_{SR}|^2 r_{SR}^{-\alpha} \Upsilon a_1}{|h_{SR}|^2 r_{SR}^{-\alpha} a_2 + I_{X_R} + I_{Y_R}}. \quad (6)$$

Since  $D_2$  has a lower power allocation,  $R$  has to decode  $D_1$  message, then decode  $D_2$  message. The SIR at  $R$  to decode  $D_2$  message, denoted  $\text{SIR}_{R_2}^{(\alpha)}$ , is expressed as <sup>2</sup>

$$\text{SIR}_{R_2}^{(\alpha)} = \frac{|h_{SR}|^2 r_{SR}^{-\alpha} \Upsilon a_2}{I_{X_R} + I_{Y_R}}. \quad (7)$$

The SIR at  $D_1$  to decode its intended message, denoted  $\text{SIR}_{D_1}^{(\alpha)}$ , is given by

$$\text{SIR}_{D_1}^{(\alpha)} = \frac{|h_{RD1}|^2 r_{RD1}^{-\alpha} \Upsilon a_1}{|h_{RD1}|^2 r_{RD1}^{-\alpha} a_2 + I_{X_{D1}} + I_{Y_{D1}}}. \quad (8)$$

In order for  $D_2$  to decode its intended message, it has to decode  $D_1$  message. The SIR at  $D_2$  to decode  $D_1$  message, denoted  $\text{SIR}_{D_{2-1}}^{(\alpha)}$ , is expressed as

$$\text{SIR}_{D_{2-1}}^{(\alpha)} = \frac{|h_{RD2}|^2 r_{RD2}^{-\alpha} \Upsilon a_1}{|h_{RD2}|^2 r_{RD2}^{-\alpha} a_2 + I_{X_{D2}} + I_{Y_{D2}}}. \quad (9)$$

The SIR at  $D_2$  to decode its intended message, denoted  $\text{SIR}_{D_2}^{(\alpha)}$ , is expressed as

$$\text{SIR}_{D_2}^{(\alpha)} = \frac{|h_{RD2}|^2 r_{RD2}^{-\alpha} \Upsilon a_2}{I_{X_{D2}} + I_{Y_{D2}}}. \quad (10)$$

### B. Outage event expressions

The outage event that  $R$  does not decode  $D_1$  message, denoted  $O_{R_1}$ , is given by

$$O_{R_1} \triangleq \bigcup_{Z \in \{\text{LOS}, \text{NLOS}\}} \left\{ Z_{SR} \cap (\text{SIR}_{R_1}^{(\alpha_Z)} < \Theta_1) \right\}, \quad (11)$$

<sup>2</sup>Perfect SIC is considered in this work, that is, no fraction of power remains after the SIC process.



where  $\Theta_1 = 2^{2\mathcal{R}_1} - 1$ , and  $\mathcal{R}_1$  is the target data rate of  $D_1$ .

Also, the outage event that  $D_1$  does not decode its intended message, denoted  $O_{D_1}$ , is given by

$$O_{D_1} \triangleq \bigcup_{Z \in \{\text{LOS}, \text{NLOS}\}} \left\{ Z_{RD_1} \cap (\text{SIR}_{D_1}^{(\alpha_Z)} < \Theta_1) \right\}, \quad (12)$$

Then, the overall outage event related to  $D_1$ , denoted  $O_{(1)}$ , is given by

$$O_{(1)} \triangleq \left[ O_{R_1} \cup O_{D_1} \right], \quad (13)$$

The outage event that  $R$  does not decode  $D_2$  message, denoted  $O_{R_2}$ , is given by

$$O_{R_2} \triangleq \bigcup_{Z \in \{\text{LOS}, \text{NLOS}\}} \bigcup_{i=1}^2 \left\{ Z_{SR} \cap (\text{SIR}_{R_i}^{(\alpha_Z)} < \Theta_i) \right\}, \quad (14)$$

where  $\Theta_2 = 2^{2\mathcal{R}_2} - 1$  ( $i = 2$ ), and  $\mathcal{R}_2$  is the target data rate of  $D_2$ . Also, the outage event that  $D_2$  does not decode its intended message, denoted  $O_{D_2}$ , is given by

$$O_{D_2} \triangleq \bigcup_{Z \in \{\text{LOS}, \text{NLOS}\}} \bigcup_{i=1}^2 \left\{ Z_{RD_2} \cap (\text{SIR}_{D_{2-i}}^{(\alpha_Z)} < \Theta_i) \right\}, \quad (15)$$

Finally, the overall outage event related to  $D_2$ , denoted  $O_{(2)}$ , is given by

$$O_{(2)} \triangleq \left[ O_{R_2} \cup O_{D_2} \right]. \quad (16)$$

### C. Outage probability expressions

In the following, we will express the outage probability related to  $O_{(1)}$  and  $O_{(2)}$ . The probability  $\mathbb{P}(O_{(1)})$  is given, when  $\Theta_1 < \frac{a_1}{a_2}$ , by (17)

$$\mathbb{P}(O_{(1)}) = 1 - \left\{ \sum_{Z \in \{\text{LOS}, \text{NLOS}\}} \mathbb{P}(Z_{SR}) \Lambda \left( \frac{m_Z \Psi_1}{\mu r_{SR}^{-\alpha_Z} \Upsilon} \right) \times \sum_{Z \in \{\text{LOS}, \text{NLOS}\}} \mathbb{P}(Z_{RD_1}) \Lambda \left( \frac{m_Z \Psi_1}{\mu r_{RD_1}^{-\alpha_Z} \Upsilon} \right) \right\}, \quad (17)$$

where  $\Psi_1 = \Theta_1 / (a_1 - \Theta_1 a_2)$ . The expression of  $\Lambda \left( \frac{m \Psi}{\mu r_{ab}^{-\alpha} \Upsilon} \right)$  is given by

$$\Lambda \left( \frac{m \Psi}{\mu r_{ab}^{-\alpha} \Upsilon} \right) = \prod_{K \in \{\text{LOS}, \text{NLOS}\}} \sum_{k=0}^{m-1} \frac{1}{k!} \left( -\frac{m \Psi}{\mu r_{ab}^{-\alpha} \Upsilon} \right)^k \sum_{n=0}^k \binom{k}{n} \frac{d^{k-n} \mathcal{L}_{I_{X_b}^K} \left( \frac{m \Psi}{\mu r_{ab}^{-\alpha} \Upsilon} \right) d^n \mathcal{L}_{I_{Y_b}^K} \left( \frac{m \Psi}{\mu r_{ab}^{-\alpha} \Upsilon} \right)}{d^{k-n} \left( \frac{m \Psi}{\mu r_{ab}^{-\alpha} \Upsilon} \right) d^n \left( \frac{m \Psi}{\mu r_{ab}^{-\alpha} \Upsilon} \right)}. \quad (18)$$

The probability  $\mathbb{P}(O_{(2)})$  is given, when  $\Theta_1 < \frac{a_1}{a_2}$ , by (19)

$$\mathbb{P}(O_{(2)}) = 1 - \left\{ \sum_{Z \in \{\text{LOS}, \text{NLOS}\}} \mathbb{P}(Z_{SR}) \Lambda \left( \frac{m_Z \Psi_{\max}}{\mu r_{SR}^{-\alpha_Z} \Upsilon} \right) \times \sum_{Z \in \{\text{LOS}, \text{NLOS}\}} \mathbb{P}(Z_{RD_2}) \Lambda \left( \frac{m_Z \Psi_{\max}}{\mu r_{RD_2}^{-\alpha_Z} \Upsilon} \right) \right\}, \quad (19)$$

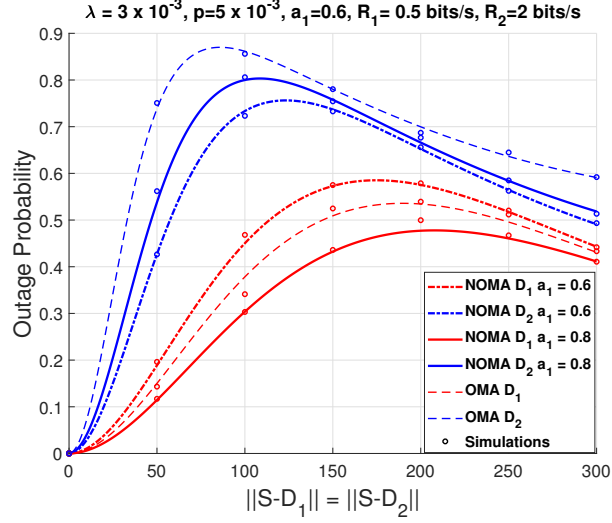


Fig. 2: Outage probability as a function of  $\|S - D_1\| = \|S - D_2\|$ . The relay  $R$  is always at mid distance between the source and the destination.

where  $\Psi_{\max} = \max(\Psi_1, \Psi_2)$ , and  $\Psi_2 = \Theta_2/a_2$ .

*Proof:* See Appendix A. ■

### III. LAPLACE TRANSFORM EXPRESSIONS

We present the Laplace transform expressions of the interference from the X road at the receiving node denoted by  $M$ , denoted  $\mathcal{L}_{I_{XM}^K}$ , and from the Y road at the receiving node denoted by  $M$ , denoted  $\mathcal{L}_{I_{YM}^K}$ . We only present the case when  $\alpha_K = 2$  due to the lack of space. The Laplace transform expressions of the interference at the node  $M$  for an intersection scenario, when  $\alpha_K = 2$  are given by

$$\mathcal{L}_{I_{XM}^K}(s) = \exp\left(\frac{-p\lambda_X^K s\pi}{\sqrt{[m \sin(\theta_M)]^2 + s}}\right), \quad (20)$$

and

$$\mathcal{L}_{I_{YM}^K}(s) = \exp\left(\frac{-p\lambda_Y^K s\pi}{\sqrt{[m \cos(\theta_M)]^2 + s}}\right). \quad (21)$$

*Proof:* See Appendix B. ■

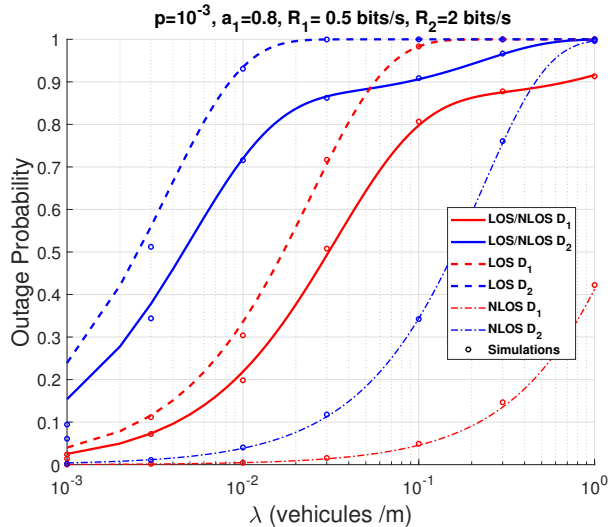


Fig. 3: Outage probability as function of  $\lambda$  considering cooperative NOMA, for LOS transmission, NLOS, and LOS/NLOS (equation) and (equation).

#### IV. SIMULATIONS AND DISCUSSIONS

In this section, we evaluate the performance of cooperative NOMA at road intersections. In order to verify the accuracy of the theoretical results, Monte Carlo simulations are obtained by averaging over 10,000 realizations of the PPPs and fading parameters. In all figures, Monte Carlo simulations are presented by marks, and they match perfectly the theoretical results, which validates the correctness of our analysis. We set, without loss of generality,  $\lambda_X^{\text{LOS}} = \lambda_Y^{\text{LOS}} = \lambda_X^{\text{NLOS}} = \lambda_Y^{\text{NLOS}} = \lambda$ .  $S = (0, 0)$ ,  $R = (50, 0)$ ,  $D_1 = (100, 10)$ ,  $D_2 = (100, -10)$ ,  $\beta = 9.5 \times 10^3$  [22],  $\mu = 1$ . We set  $\alpha_{\text{LOS}} = 2$ ,  $\alpha_{\text{NLOS}} = 4$ ,  $m_{\text{LOS}} = 2$ , and  $m_{\text{NLOS}} = 1$ .  $G_{\text{max}} = 18$  dBi,  $\eta = 30$  GHz.

Fig.2 plots the outage probability as a function of the distance between the source and the destinations. Without loss of generality, we set  $R$  at mid distance between  $S$  and the two destinations  $D_1$  and  $D_2$ . We can see that cooperative NOMA outperforms cooperative OMA when  $a_1 = 0.8$  for both  $D_1$  and  $D_2$ . However, this is not the case for  $a_1 = 0.6$ , when NOMA outperforms OMA only for  $D_2$ . This is because when  $a_1$  decreases, less power is allocated to  $D_1$ , hence it increases the outage probability. We can also see from Fig.2 that the outage probability increases until 200 m for  $D_1$  (100 m for  $D_2$ ). This because, as the distance between the transmitting and the receiving nodes increases, the probability of LOS decreases, hence decreasing the outage probability.

Fig. 3 plots the outage probability as function of  $\lambda$  considering cooperative NOMA, for

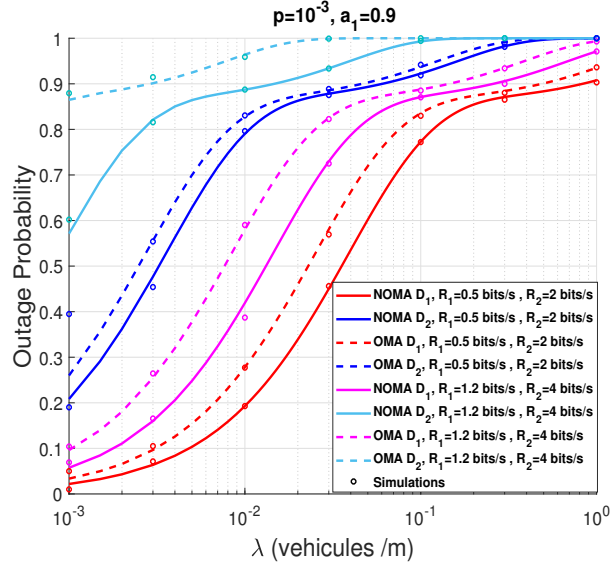


Fig. 4: Outage probability as a function of  $\lambda$  considering cooperative NOMA and cooperative OMA.

LOS transmission, NLOS, and LOS/NLOS. We can see that LOS scenario has the highest outage probability. This is because, when the interference is in direct line of sight with the set  $\{S, R, D_1, D_2\}$ , the power of aggregate interference increases, hence reducing the SIR and increasing the outage. On the other hand, the NLOS scenario has the smallest outage, since the interference is not in line of sight with the transmitting nodes. Our model is a realistic scenario, since it has LOS and NLOS between the interference, which makes its performance fall in the middle.

Fig. 4 plots the outage probability as a function of  $\lambda$  considering cooperative NOMA and cooperative OMA for several values of data rates. We can see that NOMA outperforms OMA. We can also see that  $D_1$  has a better performance than  $D_2$ . This is because  $D_1$  has a smaller target data rate, since  $D_1$  needs to be served quickly (alert message). We can notice that, as the data rates increase ( $R_1 = 1.2 \text{ bits/s}$  and  $R_2 = 4 \text{ bits/s}$ ), the performance gap between NOMA and OMA increases. This is because, as the data rates increase, the decoding threshold of OMA increases dramatically ( $\Theta_{\text{OMA}} = 2^{4R} - 1$ ). This is more relevant for  $D_2$  since it has a higher data rate than  $D_1$ , which makes cooperative NOMA a suitable candidate for vehicular communications. Fig. 5 plots the outage probability of the distance from the intersection considering cooperative NOMA and cooperative OMA, for LOS scenario and NLOS scenario. Without loss of generality, we set  $R$  at mid distance between  $S$  and the two destinations  $D_1$  and  $D_2$ . We notice from Fig. 5

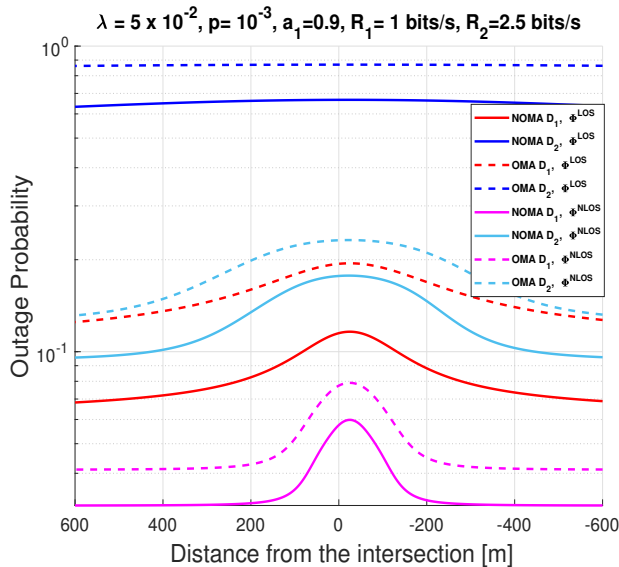


Fig. 5: Outage probability as a function of the distance from the intersection considering cooperative NOMA and cooperative OMA, for LOS scenario and NLOS scenario.

that as nodes approach the intersection, the outage probability increases. This is because when the nodes are far from the intersection, only the interferers in the same road segment contribute to the aggregate interference, but as the nodes approach the intersection, both road segments contribute to the aggregate interference. We also notice that the LOS scenario has a higher outage than the NLOS scenario. However, we can see that  $D_2$  has a severe outage in the LOS scenario compared to the NLOS scenario. We can also see that the increase in outage for  $D_2$  in the LOS scenario, as nodes move toward the intersection, is negligible. This is because, in a LOS scenario, the aggregate interference from both road segments contributes to the outage, whether the nodes are close or far from the intersection.

## V. CONCLUSION

In this paper, we studied the impact and the improvement of using cooperative non-orthogonal multiple access schemes on a mmWave vehicular network at intersection roads. The analysis was conducted using tools from stochastic geometry and was verified with Monte Carlo simulations. We derived closed-form outage probability expressions for cooperative NOMA, and compared them with cooperative OMA. We showed that cooperative NOMA exhibited a significant improvement compared to cooperative OMA, especially for high data rates. However, data rates must respect a given condition; if not, the performance of cooperative NOMA will decrease.

drastically. We also showed that as the nodes approach the intersection, the outage probability increased. Counter-intuitively, We showed that, NLOS scenario has a better performance than LOS scenario.

#### APPENDIX A

To calculate  $\mathbb{P}(O_{(1)})$ , we express it as a function of a success probability  $\mathbb{P}(O_{(1)}^C)$ , where  $\mathbb{P}(O_{D_1}^C)$  is expressed as

$$\mathbb{P}(O_{(1)}) = 1 - \mathbb{P}(O_{(1)}^C), \quad (22)$$

The probability  $\mathbb{P}(O_{(1)}^C)$  is expressed as

$$\mathbb{P}(O_{(1)}^C) = 1 - \mathbb{P}(O_{R_1}^C \cap O_{D_1}^C) = \mathbb{P}(O_{R_1}^C)\mathbb{P}(O_{D_1}^C), \quad (23)$$

where

$$O_{R_1}^C \triangleq \bigcup_{Z \in \{\text{LOS}, \text{NLOS}\}} \left\{ Z_{SR} \cap (\text{SIR}_{R_1}^{(\alpha_Z)} \geq \Theta_1) \right\} \quad (24)$$

$$O_{D_1}^C \triangleq \bigcup_{Z \in \{\text{LOS}, \text{NLOS}\}} \left\{ Z_{RD_1} \cap (\text{SIR}_{D_1}^{(\alpha_Z)} \geq \Theta_1) \right\}. \quad (25)$$

We calculate The probability  $\mathbb{P}(O_{R_1}^C)$  as

$$\begin{aligned} \mathbb{P}(O_{R_1}^C) &= \sum_{Z \in \{\text{LOS}, \text{NLOS}\}} \mathbb{E}_{I_X, I_Y} \left[ \mathbb{P} \left\{ Z_{SR} \cap (\text{SIR}_{R_1}^{(\alpha_Z)} \geq \Theta_1) \right\} \right] \\ &= \sum_{Z \in \{\text{LOS}, \text{NLOS}\}} \mathbb{P}(Z_{SR}) \mathbb{E}_{I_X, I_Y} \left[ \mathbb{P} \left\{ \text{SIR}_{R_1}^{(\alpha_Z)} \geq \Theta_1 \right\} \right] \\ &= \sum_{Z \in \{\text{LOS}, \text{NLOS}\}} \mathbb{P}(Z_{SR}) \mathbb{E}_{I_X, I_Y} \left[ \mathbb{P} \left\{ \frac{|h_{SR}|^2 r_{SR}^{-\alpha_Z} \Upsilon a_1}{|h_{SR}|^2 r_{SR}^{-\alpha_Z} \Upsilon a_2 + I_{X_R} + I_{Y_R}} \geq \Theta_1 \right\} \right] \\ &= \sum_{Z \in \{\text{LOS}, \text{NLOS}\}} \mathbb{P}(Z_{SR}) \mathbb{E}_{I_X, I_Y} \left[ \mathbb{P} \left\{ |h_{SR}|^2 r_{SR}^{-\alpha_Z} \Upsilon (a_1 - \Theta_1 a_2) \geq \Theta_1 [I_{X_R} + I_{Y_R}] \right\} \right]. \quad (26) \end{aligned}$$

We can notice from (26) that, when  $\Theta_1 \geq a_1/a_2$ , the success probability  $\mathbb{P}(O_{R_1}^C)$  is always zero, that is,  $\mathbb{P}(O_{R_1}) = 1$ . Then, when  $\Theta_1 < a_1/a_2$ , and after setting  $\Psi_1 = \Theta_1/(a_1 - \Theta_1 a_2)$ , then

$$\mathbb{P}(O_{R_1}^C) = \sum_{Z \in \{\text{LOS}, \text{NLOS}\}} \mathbb{P}(Z_{SR}) \mathbb{E}_{I_X, I_Y} \left[ \mathbb{P} \left\{ |h_{SR}|^2 \geq \frac{\Psi_1}{r_{SR}^{-\alpha_Z} \Upsilon} [I_{X_R} + I_{Y_R}] \right\} \right].$$

Since  $|h_{SR}|^2$  follows a gamma distribution, its complementary cumulative distribution function (CCDF) is given by

$$\bar{F}_{|h_{SR}|^2}(X) = \mathbb{P}(|h_{SR}|^2 > X) = \frac{\Gamma(m_Z, \frac{m_Z}{\mu} X)}{\Gamma(m_Z)}, \quad (27)$$

hence

$$\begin{aligned} \mathbb{P}(O_{R_1}^C) &= \sum_{Z \in \{\text{LOS}, \text{NLOS}\}} \mathbb{P}(Z_{SR}) \mathbb{E}_{I_X, I_Y} \left[ \frac{\Gamma\left(m_Z, \frac{m_Z \Psi_1}{\mu r_{SR}^{-\alpha_Z} \Upsilon} (I_{X_R}^{\text{LOS}} + I_{Y_R}^{\text{LOS}})\right)}{\Gamma(m_Z)} \right] \\ &\quad \times \mathbb{E}_{I_X, I_Y} \left[ \frac{\Gamma\left(m_Z, \frac{m_Z \Psi_1}{\mu r_{SR}^{-\alpha_Z} \Upsilon} (I_{X_R}^{\text{NLOS}} + I_{Y_R}^{\text{NLOS}})\right)}{\Gamma(m_Z)} \right] \\ &= \sum_{Z \in \{\text{LOS}, \text{NLOS}\}} \mathbb{P}(Z_{SR}) \prod_{K \in \{\text{LOS}, \text{NLOS}\}} \mathbb{E}_{I_X, I_Y} \left[ \frac{\Gamma\left(m_Z, \frac{m_Z \Psi_1}{\mu r_{SR}^{-\alpha_Z} \Upsilon} (I_{X_R}^K + I_{Y_R}^K)\right)}{\Gamma(m_Z)} \right] \end{aligned} \quad (28)$$

The exponential sum function when  $m_Z$  is an integer is defined as

$$e_{(m_Z)} = \sum_{k=0}^{m_Z-1} \frac{\left(\frac{m_Z}{\mu} X\right)^k}{k!} = e^X \frac{\Gamma(m_Z, \frac{m_Z}{\mu} X)}{\Gamma(m_Z)}, \quad (29)$$

then

$$\frac{\Gamma(m_Z, \frac{m_Z}{\mu} X)}{\Gamma(m_Z)} = e^{-\frac{m_Z}{\mu} X} \sum_{k=0}^{m_Z-1} \frac{1}{k!} \left(\frac{m_Z}{\mu} X\right)^k. \quad (30)$$

The expectation in equation (28) then becomes

$$\begin{aligned} &\mathbb{E}_{I_X, I_Y} \left[ \exp\left(-\frac{m_Z \Psi_1}{\mu r_{SR}^{-\alpha_Z} \Upsilon} (I_{X_R}^K + I_{Y_R}^K)\right) \times \sum_{k=0}^{m_Z-1} \frac{1}{k!} \left(\frac{m_Z \Psi_1}{\mu r_{SR}^{-\alpha_Z} \Upsilon} (I_{X_R}^K + I_{Y_R}^K)\right)^k \right] \\ &= \sum_{k=0}^{m_Z-1} \frac{1}{k!} \left(\frac{m_Z \Psi_1}{\mu r_{SR}^{-\alpha_Z} \Upsilon}\right)^k \mathbb{E}_{I_X, I_Y} \left[ \exp\left(-\frac{m_Z \Psi_1}{\mu r_{SR}^{-\alpha_Z} \Upsilon} (I_{X_R}^K + I_{Y_R}^K)\right) (I_{X_R}^K + I_{Y_R}^K)^k \right]. \end{aligned} \quad (31)$$

Applying the binomial theorem in (31), we get

$$\begin{aligned} &\sum_{k=0}^{m_Z-1} \frac{1}{k!} \left(\frac{m_Z \Psi_1}{\mu r_{SR}^{-\alpha_Z} \Upsilon}\right)^k \mathbb{E}_{I_X, I_Y} \left[ \exp\left(-\frac{m_Z \Psi_1}{\mu r_{SR}^{-\alpha_Z} \Upsilon} [I_{X_R}^K + I_{Y_R}^K]\right) \sum_{n=0}^k \binom{k}{n} (I_{X_R}^K)^{k-n} (I_{Y_R}^K)^n \right] \\ &= \sum_{k=0}^{m_Z-1} \frac{1}{k!} \Omega^k \mathbb{E}_{I_X, I_Y} \left[ \exp\left(-\Omega [I_{X_R}^K + I_{Y_R}^K]\right) \sum_{n=0}^k \binom{k}{n} (I_{X_R}^K)^{k-n} (I_{Y_R}^K)^n \right], \end{aligned} \quad (32)$$

where  $\Omega = \frac{m_Z \Psi_1}{\mu r_{SR}^{-\alpha_Z} \Upsilon}$ . To calculate the expectation in (32) we process as follows

$$\begin{aligned}
\mathbb{E}_{I_X, I_Y} \left[ e^{-\Omega I_{X_R}^K} e^{-\Omega I_{Y_R}^K} \sum_{n=0}^k \binom{k}{n} (I_{X_R}^K)^{k-n} (I_{Y_R}^K)^n \right] \\
&= \sum_{n=0}^k \binom{k}{n} \mathbb{E}_{I_X, I_Y} \left[ e^{-\Omega I_{X_R}^K} e^{-\Omega I_{Y_R}^K} (I_{X_R}^K)^{k-n} (I_{Y_R}^K)^n \right] \\
&= \sum_{n=0}^k \binom{k}{n} \mathbb{E}_{I_X} \left[ e^{-\Omega I_{X_R}^K} (I_{X_R}^K)^{k-n} \right] \mathbb{E}_{I_{Y_R}^K} \left[ e^{-\Omega I_{Y_R}^K} (I_{Y_R}^K)^n \right] \\
&\stackrel{(a)}{=} \sum_{n=0}^k \binom{k}{n} (-1)^{k-n} \frac{d^{k-n} \mathcal{L}_{I_{X_R}^K}(\Omega)}{d^{k-n} \Omega} (-1)^n \frac{d^n \mathcal{L}_{I_{Y_R}^K}(\Omega)}{d^n \Omega} \\
&= (-1)^k \sum_{n=0}^k \binom{k}{n} \frac{d^{k-n} \mathcal{L}_{I_{X_R}^K}(\Omega)}{d^{k-n} \Omega} \frac{d^n \mathcal{L}_{I_{Y_R}^K}(\Omega)}{d^n \Omega}. \tag{33}
\end{aligned}$$

where (a) stems from the following property

$$\mathbb{E}_I \left[ e^{-\Omega I} I^N \right] = (-1)^N \frac{d^N \mathbb{E}_I \left[ e^{-\Omega I} I^N \right]}{d^N \Omega} = (-1)^N \frac{d^N \mathcal{L}_I(\Omega)}{d^N \Omega}, \tag{34}$$

Finally, the expectation becomes

$$\sum_{k=0}^{m_Z-1} \frac{1}{k!} \left( -\frac{m_Z \Psi_1}{\mu r_{SR}^{-\alpha_Z} \Upsilon} \right)^k \sum_{n=0}^k \binom{k}{n} \frac{d^{k-n} \mathcal{L}_{I_{X_R}^K} \left( \frac{m_Z \Psi_1}{\mu r_{SR}^{-\alpha_Z} \Upsilon} \right)}{d^{k-n} \left( \frac{m_Z \Psi_1}{\mu r_{SR}^{-\alpha_Z} \Upsilon} \right)} \frac{d^n \mathcal{L}_{I_{Y_R}^K} \left( \frac{m_Z \Psi_1}{\mu r_{SR}^{-\alpha_Z} \Upsilon} \right)}{d^n \left( \frac{m_Z \Psi_1}{\mu r_{SR}^{-\alpha_Z} \Upsilon} \right)}. \tag{35}$$

Then plugging (35) in (28) yields

$$\begin{aligned}
\mathbb{P}(O_{R_1}^C) &= \sum_{Z \in \{\text{LOS}, \text{NLOS}\}} \mathbb{P}(Z_{SR}) \times \\
&\prod_{K \in \{\text{LOS}, \text{NLOS}\}} \sum_{k=0}^{m_L-1} \frac{1}{k!} \left( -\frac{m_Z \Psi_1}{\mu r_{SR}^{-\alpha_Z} \Upsilon} \right)^k \sum_{n=0}^k \binom{k}{n} \frac{d^{k-n} \mathcal{L}_{I_{X_R}^K} \left( \frac{m_Z \Psi_1}{\mu r_{SR}^{-\alpha_Z} \Upsilon} \right)}{d^{k-n} \left( \frac{m_Z \Psi_1}{\mu r_{SR}^{-\alpha_Z} \Upsilon} \right)} \frac{d^n \mathcal{L}_{I_{Y_R}^K} \left( \frac{m_Z \Psi_1}{\mu r_{SR}^{-\alpha_Z} \Upsilon} \right)}{d^n \left( \frac{m_Z \Psi_1}{\mu r_{SR}^{-\alpha_Z} \Upsilon} \right)} \tag{36}
\end{aligned}$$

The expression of  $d^{k-n} \mathcal{L}_{I_X^K}(s)/d^{k-n}(s)$  and  $d^n \mathcal{L}_{I_Y^K}(s)/d^n(s)$  are given by (52) and (53). The probability  $\mathbb{P}(O_{D_1}^C)$  can be calculated following the same steps above.

In the same way we express  $\mathbb{P}(O_{(2)})$  as a function of a success probability  $\mathbb{P}(O_{(2)}^C)$ , where  $\mathbb{P}(O_{(2)}^C)$  is given by

$$\mathbb{P}(O_{(2)}) = 1 - \mathbb{P}(O_{(2)}^C). \tag{37}$$



The probability  $\mathbb{P}(O_{(2)}^C)$  is expressed as

$$\mathbb{P}(O_{(2)}^C) = 1 - \mathbb{P}(O_{R_2}^C \cap O_{D_2}^C) = \mathbb{P}(O_{R_2}^C)\mathbb{P}(O_{D_2}^C), \quad (38)$$

where

$$O_{R_2}^C \triangleq \bigcup_{Z \in \{\text{LOS}, \text{NLOS}\}} \bigcap_{i=1}^2 \left\{ Z_{SR} \cap (\text{SIR}_{R_i}^{(\alpha_Z)} \geq \Theta_i) \right\} \quad (39)$$

$$O_{D_2}^C \triangleq \bigcup_{Z \in \{\text{LOS}, \text{NLOS}\}} \bigcap_{i=1}^2 \left\{ Z_{RD_2} \cap (\text{SIR}_{D_{2-i}}^{(\alpha_Z)} < \Theta_i) \right\}. \quad (40)$$

To calculate  $\mathbb{P}(O_{R_2}^C)$  we proceed as follows

$$\begin{aligned} \mathbb{P}(O_{R_2}^C) &= \sum_{Z \in \{\text{LOS}, \text{NLOS}\}} \mathbb{E}_{I_X, I_Y} \left[ \mathbb{P} \left\{ \bigcap_{i=1}^2 \left\{ Z_{SR} \cap (\text{SIR}_{R_i}^{(\alpha_Z)} \geq \Theta_i) \right\} \right\} \right] \\ &= \sum_{Z \in \{\text{LOS}, \text{NLOS}\}} \mathbb{P}(Z_{SR}) \mathbb{E}_{I_X, I_Y} \left[ \mathbb{P} \left\{ \bigcap_{i=1}^2 \text{SIR}_{R_i}^{(\alpha_Z)} \geq \Theta_i \right\} \right] \\ &= \sum_{Z \in \{\text{LOS}, \text{NLOS}\}} \mathbb{P}(Z_{SR}) \mathbb{E}_{I_X, I_Y} \left[ \mathbb{P} \left\{ \text{SIR}_{R_1}^{(\alpha_Z)} \geq \Theta_1 \cap \text{SIR}_{R_2}^{(\alpha_Z)} \geq \Theta_2 \right\} \right]. \end{aligned}$$

Following the same steps as for  $\mathbb{P}(O_{R_1}^C)$ , we get

$$\mathbb{P}(O_{R_2}^C) = \mathbb{E}_{I_X, I_Y} \left[ \mathbb{P} \left\{ \frac{|h_{SR}|^2 r_{SR}^{-\alpha_Z} \Upsilon a_1}{|h_{SR}|^2 r_{SR}^{-\alpha_Z} \Upsilon a_2 + I_{X_R} + I_{Y_R}} \geq \Theta_1, \frac{|h_{SR}|^2 r_{SR}^{-\alpha_Z} \Upsilon a_2}{I_{X_R} + I_{Y_R}} \geq \Theta_2 \right\} \right].$$

When  $\Theta_1 > a_1/a_2$ , then  $\mathbb{P}(O_{R_2}) = 1$ , otherwise we continue the derivation We set  $\Psi_2 = \Theta_2/a_2$ , then

$$\begin{aligned} \mathbb{P}(O_{R_2}^C) &= \mathbb{E}_{I_X, I_Y} \left[ \mathbb{P} \left\{ |h_{SR}|^2 \geq \frac{\Psi_1}{r_{SR}^{-\alpha_Z} \Upsilon} [I_{X_R} + I_{Y_R}], |h_{SR}|^2 \geq \frac{\Psi_2}{r_{SR}^{-\alpha_Z} \Upsilon} [I_{X_R} + I_{Y_R}] \right\} \right] \\ &= \mathbb{E}_{I_X, I_Y} \left[ \mathbb{P} \left\{ |h_{SR}|^2 \geq \frac{\max(\Psi_1, \Psi_2)}{r_{SR}^{-\alpha_Z} \Upsilon} [I_{X_R} + I_{Y_R}] \right\} \right]. \end{aligned}$$

Following the same steps above,  $\mathbb{P}(O_{R_2}^C)$  equals

$$\begin{aligned} \mathbb{P}(O_{R_2}^C) &= \sum_{Z \in \{\text{LOS}, \text{NLOS}\}} \mathbb{P}(Z_{SR}) \times \\ &\prod_{K \in \{\text{LOS}, \text{NLOS}\}} \sum_{k=0}^{m_L-1} \frac{1}{k!} \left( -\frac{m_Z \Psi_{\max}}{\mu r_{SR}^{-\alpha_Z} \Upsilon} \right)^k \sum_{n=0}^k \binom{k}{n} \frac{d^{k-n} \mathcal{L}_{I_{X_R}^k} \left( \frac{m_Z \Psi_{\max}}{\mu r_{SR}^{-\alpha_Z} \Upsilon} \right) d^n \mathcal{L}_{I_{Y_R}^k} \left( \frac{m_Z \Psi_{\max}}{\mu r_{SR}^{-\alpha_Z} \Upsilon} \right)}{d^{k-n} \left( \frac{m_Z \Psi_{\max}}{\mu r_{SR}^{-\alpha_Z} \Upsilon} \right) d^n \left( \frac{m_Z \Psi_{\max}}{\mu r_{SR}^{-\alpha_Z} \Upsilon} \right)} \end{aligned} \quad (41)$$

where  $\Psi_{\max} = \max(\Psi_1, \Psi_2)$ . The probability  $\mathbb{P}(O_{D_2}^C)$  can be calculated following the same steps above.

## APPENDIX B

The Laplace transform of the interference originating from the X road at  $M$  is expressed as

$$\begin{aligned}
\mathcal{L}_{I_{X_M}^K}(s) &= \mathbb{E} \left[ \exp \left( -s I_{X_M}^K \right) \right] \\
&= \mathbb{E} \left[ \exp \left( - \sum_{x \in \Phi_{X_M}^K} s |h_{Mx}|^2 r_{Mx}^{-\alpha_K} \right) \right] \\
&= \mathbb{E} \left[ \prod_{x \in \Phi_{X_M}^K} \exp \left( -s |h_{Mx}|^2 r_{Mx}^{-\alpha_K} \right) \right] \\
&\stackrel{(a)}{=} \mathbb{E} \left[ \prod_{x \in \Phi_{X_M}^K} \mathbb{E}_{|h_{Mx}|^2, p} \left\{ \exp \left( -s |h_{Mx}|^2 r_{Mx}^{-\alpha_K} \right) \right\} \right] \\
&\stackrel{(b)}{=} \mathbb{E} \left[ \prod_{x \in \Phi_{X_M}^K} \frac{p}{1 + s r_{Mx}^{-\alpha_K}} + 1 - p \right] \\
&\stackrel{(c)}{=} \exp \left( -\lambda_X^K \int_{\mathbb{R}} \left[ 1 - \left( \frac{p}{1 + s r_{Mx}^{-\alpha_K}} + 1 - p \right) \right] dx \right) \\
&= \exp \left( -p \lambda_X^K \int_{\mathbb{R}} \frac{1}{1 + 1/s r_{Mx}^{-\alpha_K}} dx \right) \tag{42}
\end{aligned}$$

$$= \exp \left( -p \lambda_X^K \int_{\mathbb{R}} \frac{1}{1 + r_{Mx}^{\alpha_K}/s} dx \right), \tag{43}$$

where (a) follows from the independence of the fading coefficients; (b) follows from performing the expectation over  $|h_{Mx}|^2$  which follows an exponential distribution with unit mean, and performing the expectation over the set of interferes; (c) follows from the probability generating functional (PGFL) of a PPP. The expression of  $\mathcal{L}_{I_{Y_M}^K}(s)$  can be acquired by following the same steps. The Laplace transform of the interference originating from the X road at the received node denoted  $M$ , is expressed as

$$\mathcal{L}_{I_{X_M}^K}(s) = \exp \left( -p \lambda_X^K \int_{\mathbb{R}} \frac{1}{1 + \|x - M\|^{\alpha_K}/s} dx \right), \tag{44}$$

where

$$\|x - M\| = \sqrt{\left[ m \sin(\theta_M) \right]^2 + \left[ x - m \cos(\theta_M) \right]^2}. \tag{45}$$

The Laplace transform of the interference originating from the Y road at  $M$  is given by

$$\mathcal{L}_{I_{YM}^K}(s) = \exp\left(-p\lambda_Y^K \int_{\mathbb{R}} \frac{1}{1 + \|y - M\|^{\alpha_K}/s} dy\right), \quad (46)$$

where

$$\|y - M\| = \sqrt{\left[m \cos(\theta_M)\right]^2 + \left[y - m \sin(\theta_M)\right]^2}, \quad (47)$$

where  $\theta_M$  is the angle between the node  $M$  and the X road.

In order to calculate the Laplace transform of interference originated from the X road at the node  $M$ , we have to calculate the integral in (44). We calculate the integral in (44) for  $\alpha_K = 2$ . Let us take  $m_x = m \cos(\theta_M)$ , and  $m_y = m \sin(\theta_M)$ , then (44) becomes

$$\begin{aligned} \mathcal{L}_{I_{XM}^K}(s) &= \exp\left(-p\lambda_X^K \int_{\mathbb{R}} \frac{1}{1 + m_y^2 + (x - m_x)^2/s} dx\right), \\ &= \exp\left(-p\lambda_X^K s \int_{\mathbb{R}} \frac{1}{s + m_y^2 + (x - m_x)^2} dx\right), \end{aligned} \quad (48)$$

and the integral inside the exponential in (48) equals

$$\int_{\mathbb{R}} \frac{1}{s + m_y^2 + (x - m_x)^2} dx = \frac{\pi}{\sqrt{m_y^2 + s}}. \quad (49)$$

Then, plugging (49) into (48), and substituting  $m_y$  by  $m \sin(\theta_M)$  we obtain

$$\mathcal{L}_{I_{XM}^K}(s) = \exp\left(-\frac{p\lambda_X^K s \pi}{\sqrt{m^2 \sin^2(\theta_M) + s}}\right). \quad (50)$$

Following the same steps above, and without details for the derivation with respect to  $s$ , we obtain

$$\mathcal{L}_{I_{YM}^K}(s) = \exp\left(-\frac{p\lambda_Y^K s \pi}{\sqrt{m^2 \cos^2(\theta_M) + s}}\right). \quad (51)$$

Then, when compute the derivative of (50) and (51), we obtain

$$\begin{aligned} \frac{d^{k-n} \mathcal{L}_{I_{XM}^K}(s)}{d^{k-n} s} &= \left[ -\frac{p\lambda_X^K \pi}{\sqrt{m^2 \sin^2(\theta_M) + s}} + \frac{1}{2} \frac{p\lambda_X^K \pi s}{(m^2 \sin^2(\theta_M) + s)^{3/2}} \right]^{k-n} \\ &\quad \times \exp\left(-\frac{p\lambda_X^K \pi s}{\sqrt{m^2 \sin^2(\theta_M) + s}}\right). \end{aligned} \quad (52)$$

$$\frac{d^n \mathcal{L}_{I_{Y_M}^K}(s)}{d^n s} = \left[ -\frac{p\lambda_Y^K \pi}{\sqrt{m^2 \cos(\theta_M)^2 + s}} + \frac{1}{2} \frac{p\lambda_Y^K \pi s}{(m^2 \cos(\theta_M)^2 + s)^{3/2}} \right]^n \times \exp\left(-\frac{p\lambda_Y^K \pi s}{\sqrt{m^2 \cos(\theta_M)^2 + s}}\right). \quad (53)$$

## REFERENCES

- [1] U.S. Dept. of Transportation, National Highway Traffic Safety Administration, "Traffic safety facts 2015," Jan. 2017.
- [2] Z. Ding, Y. Liu, J. Choi, Q. Sun, M. Elkashlan, I. Chih-Lin, and H. V. Poor, "Application of non-orthogonal multiple access in lte and 5g networks," *IEEE Communications Magazine*, vol. 55, no. 2, pp. 185–191, 2017.
- [3] W. Roh, J.-Y. Seol, J. Park, B. Lee, J. Lee, Y. Kim, J. Cho, K. Cheun, and F. Aryanfar, "Millimeter-wave beamforming as an enabling technology for 5g cellular communications: Theoretical feasibility and prototype results," *IEEE communications magazine*, vol. 52, no. 2, pp. 106–113, 2014.
- [4] Y. Saito, Y. Kishiyama, A. Benjebbour, T. Nakamura, A. Li, and K. Higuchi, "Non-orthogonal multiple access (noma) for cellular future radio access," in *Vehicular Technology Conference (VTC Spring), 2013 IEEE 77th*. IEEE, 2013, pp. 1–5.
- [5] L. Dai, B. Wang, Y. Yuan, S. Han, I. Chih-Lin, and Z. Wang, "Non-orthogonal multiple access for 5g: solutions, challenges, opportunities, and future research trends," *IEEE Communications Magazine*, vol. 53, no. 9, pp. 74–81, 2015.
- [6] S. R. Islam, N. Avazov, O. A. Dobre, and K.-S. Kwak, "Power-domain non-orthogonal multiple access (noma) in 5g systems: Potentials and challenges," *IEEE Communications Surveys & Tutorials*, vol. 19, no. 2, pp. 721–742, 2017.
- [7] Z. Ding, Z. Yang, P. Fan, and H. V. Poor, "On the performance of non-orthogonal multiple access in 5g systems with randomly deployed users," *IEEE Signal Processing Letters*, vol. 21, no. 12, pp. 1501–1505, 2014.
- [8] Z. Mobini, M. Mohammadi, H. A. Suraweera, and Z. Ding, "Full-duplex multi-antenna relay assisted cooperative non-orthogonal multiple access," *arXiv preprint arXiv:1708.03919*, 2017.
- [9] K. S. Ali, H. ElSawy, A. Chaaban, M. Haenggi, and M.-S. Alouini, "Analyzing non-orthogonal multiple access (noma) in downlink poisson cellular networks," in *Proc. of IEEE International Conference on Communications (ICC18)*, 2018.
- [10] Z. Zhang, H. Sun, R. Q. Hu, and Y. Qian, "Stochastic geometry based performance study on 5g non-orthogonal multiple access scheme," in *Global Communications Conference (GLOBECOM), 2016 IEEE*. IEEE, 2016, pp. 1–6.
- [11] H. Tabassum, E. Hossain, and J. Hossain, "Modeling and analysis of uplink non-orthogonal multiple access in large-scale cellular networks using poisson cluster processes," *IEEE Transactions on Communications*, vol. 65, no. 8, pp. 3555–3570, 2017.
- [12] Y. Liu, Z. Qin, M. Elkashlan, A. Nallanathan, and J. A. McCann, "Non-orthogonal multiple access in large-scale heterogeneous networks," *IEEE Journal on Selected Areas in Communications*, vol. 35, no. 12, pp. 2667–2680, 2017.
- [13] S. Biswas, S. Vuppala, J. Xue, and T. Ratnarajah, "On the performance of relay aided millimeter wave networks," *IEEE Journal of Selected Topics in Signal Processing*, vol. 10, no. 3, pp. 576–588, 2016.
- [14] S. Wu, R. Atat, N. Mastrorade, and L. Liu, "Coverage analysis of d2d relay-assisted millimeter-wave cellular networks," in *2017 IEEE Wireless Communications and Networking Conference (WCNC)*. IEEE, 2017, pp. 1–6.
- [15] K. Belbase, C. Tellambura, and H. Jiang, "Two-way relay selection for millimeter wave networks," *IEEE Communications Letters*, vol. 22, no. 1, pp. 201–204, 2018.
- [16] K. Belbase, Z. Zhang, H. Jiang, and C. Tellambura, "Coverage analysis of millimeter wave decode-and-forward networks with best relay selection," *IEEE Access*, vol. 6, pp. 22 670–22 683, 2018.
- [17] A. Tassi, M. Egan, R. J. Piechocki, and A. Nix, "Modeling and design of millimeter-wave networks for highway vehicular communication," *IEEE Transactions on Vehicular Technology*, vol. 66, no. 12, pp. 10 676–10 691, 2017.

- [18] E. Steinmetz, M. Wildemeersch, T. Q. Quek, and H. Wymeersch, "A stochastic geometry model for vehicular communication near intersections," in *Globecom Workshops (GC Wkshps), 2015 IEEE*. IEEE, 2015, pp. 1–6.
- [19] M. Abdulla, E. Steinmetz, and H. Wymeersch, "Vehicle-to-vehicle communications with urban intersection path loss models," in *Globecom Workshops (GC Wkshps), 2016 IEEE*. IEEE, 2016, pp. 1–6.
- [20] J. P. Jeyaraj and M. Haenggi, "Reliability analysis of v2v communications on orthogonal street systems," in *GLOBECOM 2017-2017 IEEE Global Communications Conference*. IEEE, 2017, pp. 1–6.
- [21] T. Kimura and H. Saito, "Theoretical interference analysis of inter-vehicular communication at intersection with power control," *Computer Communications*, 2017.
- [22] T. Bai, R. Vaze, and R. W. Heath, "Analysis of blockage effects on urban cellular networks," *IEEE Transactions on Wireless Communications*, vol. 13, no. 9, pp. 5070–5083, 2014.
- [23] Z. Ding, H. Dai, and H. V. Poor, "Relay selection for cooperative noma," *IEEE Wireless Communications Letters*, vol. 5, no. 4, pp. 416–419, 2016.
- [24] Z. Ding, L. Dai, and H. V. Poor, "Mimo-noma design for small packet transmission in the internet of things," *IEEE access*, vol. 4, pp. 1393–1405, 2016.
- [25] S. Singh, M. N. Kulkarni, A. Ghosh, and J. G. Andrews, "Tractable model for rate in self-backhauled millimeter wave cellular networks," *IEEE Journal on Selected Areas in Communications*, vol. 33, no. 10, pp. 2196–2211, 2015.
- [26] M. O. Hasna, M.-S. Alouini, A. Bastami, and E. S. Ebbini, "Performance analysis of cellular mobile systems with successive co-channel interference cancellation," *IEEE Transactions on Wireless Communications*, vol. 2, no. 1, pp. 29–40, 2003.